Observations of a Circular, Triple-Helical Polysaccharide Using Noncontact Atomic Force Microscopy

Theresa M. McIntire, Reginald M. Penner, and David A. Brant*

Department of Chemistry, University of California, Irvine, Irvine, California 92717-2025

Received April 20, 1995
Revised Manuscript Received June 26, 1995

Introduction. Unmodifed biopolymer samples dispersed on atomically flat substrate surfaces have been imaged at molecular resolution in gaseous ambients[1-3] and in aqueous electrolyte solutions[1,3-5] using atomic force microscopy (AFM).[6] Successful implementation of AFM for investigations of biopolymers has required methods for preventing the displacement of polymer molecules under the influence of the scanning probe tip. In the AFM investigations of DNA structure reported by Bustamante and co-workers,[2] for example, negatively charged DNA strands were anchored electrostatically to a positively charged mica surface in the Mg^{2+} form.

Recently noncontact atomic force microscopy (NCAFM, also called dynamic force microscopy)[7-12] has permitted nondestructive imaging of particularly soft biological surfaces. In conventional AFM the vertical position of the probe tip is established by sensing the short-range, repulsive portion of the interaction potential with the surface. In the NCAFM experiment a sharpened silicon tip mounted on a cantilever spring is mechanically excited at its resonance frequency. The amplitude and frequency of tip oscillation are affected when the tip approaches the sample surface through intervention of the *attractive* intermolecular forces. In comparison with conventional repulsive-mode AFM, this attractive interaction occurs at relatively large tip-to-sample distances (10–100 Å). Either the amplitude or frequency of the tip vibrations is monitored and maintained constant during rastering by adjusting the distance separating the tip from the sample surface. The long-range attractive forces involved in NCAFM imaging are much weaker than the repulsive forces measured in conventional AFM with the result that adsorbed molecules are not swept away, damaged, or deformed.

Most prior scanning probe microscopy studies of polysaccharides have employed scanning tunneling microscopy (STM) and have achieved limited resolution.[13-21] Among the remaining applications of scanning probe microscopy to polysaccharides[6,22-26] many do not report individual molecular images. In two cases AFM images presented were of continuous two-dimensional periodic arrays rather than images of individual molecules showing chain ends or defects.[24,25] While information on crystalline structures and molecular cross sections may be available from such images, molecular attributes such as molecular weight, molecular flexibility, and helical defect structures are not accessible. Recently Kirby et al.[26] have reported molecularly resolved images of xanthan molecules on freshly cleaved mica under liquid.

Here we describe application of the NCAFM technique to achieve molecular resolution images of the immunostimulatory[27,28] (1→6)-branched β-(1→3)-D-glucan scleroglucan (also known as schizophyllan).[29,30] Sample preparation involves deposition of the polysaccharide molecules from an aqueous solution onto a freshly cleaved and atomically smooth mica surface by spraying and air drying. Because the forces between the NCAFM probe tip and the biopolymer sample are comparable to those between the polymer chain and the mica surface, no special immobilization of the polymer is necessary, and stable, molecular-resolution NCAFM images of physisorbed polymer molecules are obtained. High-resolution (i.e., ≈1 Å vertical, 50 Å lateral) NCAFM images have been obtained in air from which the mean polymer chain length (and molar mass) and the mean chain diameter have been estimated from measurements on a sizable sample of molecules. These results can be compared with similar measurements on schizophyllan using transmission electron microscopy (TEM).[31-33]

The conformation and morphology of (1→6)-branched (1→3)-β-D-glucans of fungal origin are of interest, both for the anticancer[27,28] activity and the stiffness of the triple-stranded native helical structure.[29,30,34,35] It has recently been discovered that these very stiff triple-stranded helical molecules can be dissociated into three random-coil chains and subsequently renatured as triple strands in linear and circular forms.[36-38] At true thermodynamic equilibrium clusters containing just three chains are expected to dominate both the linear and circular helical components in the renatured samples.[38] The existence of the circular structures was quite unexpected given the stiff nature of the linear triple helix.[37] The circles are reminiscent of circular DNA,[39] and they also display twisted or supercoiled forms[40] arising from torsional stress in the helical backbone, although the scleroglucan circles are not covalently closed.[36] We show here that the linear-triple-helix ↔ circular-triple-helix transformation previously observed in TEM[36-38] can also be studied using NCAFM.

Experimental Section. Scleroglucan (Actigum CS 6, Ceca S. A., France) was dissolved at 5 g/L in aqueous 0.02% NaN_3, sonicated (20 kHz, 375 W, ½ in. tip) at 0 °C for 3 h, and centrifuged and filtered to remove particulates. The resulting solution was then fractionally precipitated[41] with isopropyl alcohol or acetone to produce 10 fractions. Each of the fractions was redissolved in water, dialyzed exhaustively against distilled water, and recovered by freeze drying. Fractions chosen for study were redissolved in water at 1 mg/mL.

Some of the redissolved samples were subjected to a denaturation–renaturation procedure: Aliquots in sealed 10-mL micro-reaction vials were first heated to 160 °C for 10 min to disrupt the native triple helix.[42] These vials were then annealed at 70 °C for 23 h and finally quenched to room temperature in an ice bath. The annealing temperature was chosen to be within the region of stability of the native triple helix but high enough to reduce kinetic hindrances to reassembly and reorganization of the triple helix.[42] The scleroglucan fractions, including samples subjected to the denaturation–renaturation procedures and those not so treated, were then diluted by a factor of 100, and 50 μL of the resulting solutions was pipetted into an atomizer which delivers a fine aerosol onto a freshly cleaved mica surface.[43] After drying in air for a few hours, the samples were imaged by NCAFM.

Scanning probe microscope images were obtained using an AutoProbe CP probe microscope (Park Scientific Instruments, Sunnyvale, CA) equipped with a noncontact AFM probe head. The tips used were V-shaped silicon 2-μm cantilevers (Ultralevers Model

* To whom correspondence should be addressed.

0024-9297/95/2228-6375$09.00/0

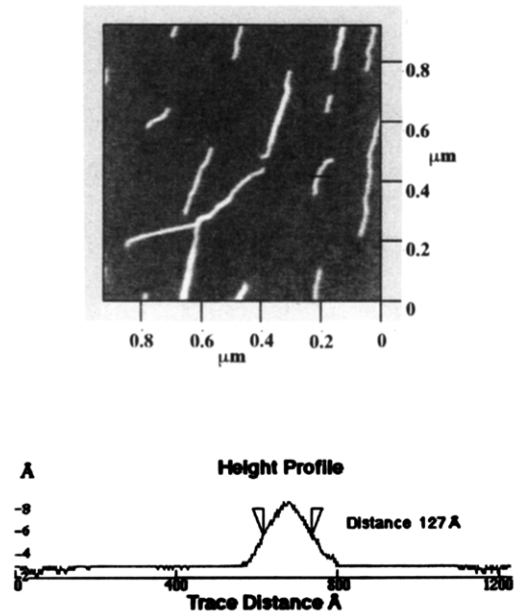

Figure 1. (a) NCAFM image of native aqueous scleroglucan fraction P-3 deposited on a mica substrate. Sample prepared as described in the text. Horizontal scale shown along bottom and right axis. (b) Trace taken along solid black line running approximately left → right in a and intersecting one scleroglucan chain: the apparent chain thickness in the dimension normal to the substrate is shown on the vertical axis, approximately 9 Å, and between wedged-shaped markers in the horizontal direction, 127 Å.

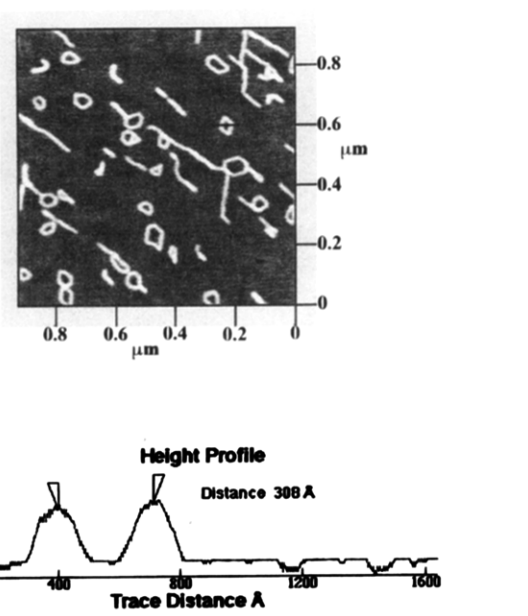

Figure 2. (a) NCAFM image of aqueous scleroglucan fraction P-3 deposited on a mica substrate following denaturation–renaturation. Sample prepared as described in the text. Horizontal scales shown as in Figure 1a. (b) Trace taken along the solid black line running left → right in a across one isolated scleroglucan circle; the apparent chain thickness in the dimension normal to the substrate is shown on the vertical axis. The selected circle has a diameter of 30.8 nm, as measured between the peak maxima.

No. APUL-20-AU-25) with a force constant of 13 N/m and resonant frequency of approximately 300 kHz. Imaging was carried out in air at a constant vibration amplitude. Images were stored as 512 × 512 point arrays.

Results and Discussion. A representative NCAFM image of sonicated and fractionated scleroglucan (fraction P-3) in its native triple-helical form is shown in Figure 1a. Individual scleroglucan molecules are clearly resolved in this image. From *ca.* 40 NCAFM images of some 250 individual scleroglucan chains, acquired over the course of several weeks and using different Ultralevers, the number-average chain length has been determined to be 189 ± 97 nm. Invoking the known linear atomic mass density of the scleroglucan helix (2140 nm^{-1}),[29] we find $M_n = (4.15 \pm 1.71) \times 10^5$. The distribution of lengths yields $M_w/M_n = 1.26$ and provides a measure of the effectiveness of the fractional precipitation procedure.

From the same data set the average chain width (measured in the direction normal to the long axis of the chain and parallel to the mica surface) and chain height (measured in the direction normal to the surface) are 18 ± 7 and 0.80 ± 0.5 nm, respectively. A sample height profile corresponding to the trace indicated in Figure 1a is shown in Figure 1b. We take the measured mean height to be a faithful reflection of the thickness of the native triple-stranded helix. Crystallographic studies of scleroglucan fibers[44] suggest, however, a triple-helix diameter of *ca.* 17 Å. Failure of the present height measurements to reproduce this dimension exactly may be related in part to the presence of one or more layers of water on the mica surface adjacent to the adsorbed macromolecule.[45] Other investigators have reported similar discrepancies between macromolecular thicknesses measured by scanning probe microscopy and the dimensions expected from independent information.[46] Other possible explanations for the observed discrepancy are that the polysaccharide molecules are deformed because of spreading and flattening that may occur upon drying of the sample and adhesion to the mica surface.

The measured mean width provides, in effect, a measure of the thickness of the probe tip, averaged over the several tips used to accumulate the data, convoluted with the *ca.* 17 Å thickness of the scleroglucan triple helix. The alignment of the molecules evident in the image may be due to ordering of the polymer chains along the crystal planes of the mica surface or perhaps to orientation effects associated with evaporation of the solvent.[31] These orientation effects serve to exaggerate the stiffness of the scleroglucan triple helix. Underlying mica surface structure possibly related to the observed macromolecular alignment cannot be observed with NCAFM.

Figure 2a shows an NCAFM image of the same scleroglucan fraction after having been subjected to the denaturation–renaturation process. A mixture of linear and cyclic structures plus several possible hairpin structures is observed. The mean diameter of some 155 circles appearing in 12 separate NCAFM images is 33 ± 12 nm, corresponding to a mean circumference of 104 nm and $M_n = (2.22 \pm 0.26) \times 10^5$ for the circles, assuming the same linear mass density as for the linear scleroglucan triple helix. For the sampled group of circles $M_w/M_n = 1.13$. We do not know at this point why M_n for the circles in the renatured sample is smaller than that for the undenatured starting material. It may simply reflect sampling error, or it may result from degradation of the single strands during the heating procedure or reflect the probability distribution for circle formation as a function of single-strand chain length.[37]

Figure 2b shows a cross section of the height profile corresponding to the indicated circle shown in Figure 2a. The measured height and width dimensions of the linear and circular components of the renatured sample (Figure 2a) are approximately the same, and they agree closely with those of the undenatured triple helix of scleroglucan reported in Figure 1. The average length of the linear structures in renatured samples is 85.7 nm, less than half the mean length before denaturation. This, coupled with the mean circumference of the circles in the renatured samples, strongly suggests that some chain degradation accompanies the thermal denaturation of the native linear triple helices.

Summary. Atomic force microscopy operating in the attractive, or noncontact, mode is used to image individual triple-helical scleroglucan molecules on a mica surface in air. The long-range attractive forces involved in NCAFM imaging are much weaker than the repulsive forces measured in conventional AFM with the result that adsorbed molecules are not swept away, damaged, or deformed. Because the interaction forces between the NCAFM tip and the biopolymer sample are approximately equal to the van der Waals attractive forces between the polymer chain and the mica surface, no special immobilization of the polymer to the substrate is required, and molecular-resolution imaging of physisorbed polymer molecules is possible. Heavy metal shadowing required for TEM imaging and metal coating needed for application of STM on the mica substrate are both unnecessary. Time and expense are thereby saved, and possible artifacts associated with application of metal are avoided. Samples may be prepared in pure water without addition of glycerol or salts, and they may be imaged in air without the need for high-vacuum equipment. Using this NCAFM technique we have been able to monitor the linear-triple-helix to circular-triple-helix transition in scleroglucan quickly, routinely, and reproducibly.

Acknowledgment. This work has been supported by NIH Research Grant GM 33062 to D.A.B., by NIH Traineeship GM 07311 to T.M.M., and by the ONR Grant 400X119YIP to R.M.P. We thank Park Scientific Instruments for donation of some of the cantilevers used in this study. T.M.M. gratefully acknowledges Dr. Mike D. Kirk at Park Scientific Instruments for valuable discussions concerning this work.

References and Notes

(1) Engel, A. *Annu. Rev. Biophys. Biophys. Chem.* **1991**, *20*, 79–108.
(2) Bustamante, C.; Vesenka, J.; Tang, C. L.; Rees, W.; Guthod, M.; Keller, R. *Biochemistry* **1992**, *31*, 22–26.
(3) Lindsay, S. M. In *Scanning Tunneling Microscopy: Theory, Techniques and Applications*; Bonnell, D. A., Ed.; VCH Press: New York, 1993.
(4) Drake, B.; Prater, C. B.; Weisenhorn, A. L.; Gould, S. A. C.; Albrecht, T. R.; Quate, C. F.; Cannell, D. S.; Hansma, H. G.; Hansma, P. K. *Science* **1989**, *243*, 1586–1589.
(5) Hansma, H. G.; Weisenhorn, A. L.; Edmundson, A. B.; Gaub, H. E.; Hansma, P. K. *Clin. Chem.* **1991**, *37*, 1497–1501.
(6) Binnig, G.; Quate, C. F.; Gerber, Ch. *Phys. Rev. Lett.* **1986**, *56*, 930–933.
(7) Martin, Y.; Williams, C. C.; Wickramasinghe, H. K. *J. Appl. Phys.* **1987**, *61*, 4723–4729.
(8) Nonnenmacher, M.; Greschner, J.; Wolter, O.; Kassing, R. *J. Vac. Sci. Technol. B* **1991**, *9*, 1358–1362.
(9) Giles, R.; Cleveland, J. P.; Manne, S.; Hansma, P. K.; Drake, B.; Maivald, P.; Boles, C.; Gurley, J.; Elings, V. *Appl. Phys. Lett.* **1993**, *63*, 617–618.
(10) Anselmetti, D.; Dreier, M.; Lüthi, R.; Richmond, T.; Meyer, E.; Frommer, J.; Güntherodt, H.-J. *J. Vac. Sci. Technol. B* **1994**, *12*, 1500–1503.
(11) Lüthi, R.; Meyer, E.; Howald, L.; Haefke, H.; Anselmetti, D.; Dreier, M.; Rüetschi, M.; Bonner, T.; Overney, R. M.; Frommer, J.; Güntherodt, H.-J. *J. Vac. Sci. Technol. B* **1994**, *12*, 1673–1676.
(12) Giessibl, F. J. *Science* **1995**, *267*, 68–71.
(13) Rabe, J. P.; Buchholz, S.; Ritcey, A. M. *J. Vac. Sci. Technol. A* **1990**, *8*, 679–683.
(14) Yang, X.; Miller, M. A.; Yang, R.; Evans, D. F.; Edstrom, R. D. *FASEB J.* **1990**, *4*, 3140–3143.
(15) Miles, M. J.; Lee, I.; Atkins, E. D. T. *J. Vac. Sci. Technol. B* **1991**, *9*, 1206–1209.
(16) Shigekawa, H.; Morozumi, T.; Komiyama, M.; Yoshimura, M.; Kawazu, A.; Saito, Y. *J. Vac. Sci. Technol. B* **1991**, *9*, 1189–1192.
(17) Lee, I.; Atkins, E. D. T.; Miles, M. J. *Ultramicroscopy* **1992**, *42–44*, 1107–1112.
(18) Oka, Y.; Takahashi, A. *Kobunshi Ronbunshu* **1992**, *49*, 389–391.
(19) Gunning, A. P.; McMaster, T. J.; Morris, V. J. *Carbohydr. Polym.* **1993**, *21*, 47–51.
(20) Wilkins, M. J.; Davies, M. C.; Jackson, D. E.; Mitchell, J. R.; Roberts, C. J.; Stokke, B. T.; Tendler, S. J. B. *Ultramicroscopy* **1993**, *48*, 197–210.
(21) Wilkins, M. J.; Davies, M. C.; Jackson, D. E.; Roberts, C. J.; Tendler, S. J. B. *J. Microsc.* **1993**, *172*, 215–221.
(22) Couso, R. O.; Ielpi, L.; Dankert, M. A. *J. Gen. Microbiol.* **1987**, *133*, 2123–2135.
(23) Hanley, S. J.; Giasson, J.; Revol, J. F.; Gray, D. G. *Polymer* **1992**, *33*, 4639–4642.
(24) Meyer, A.; Rouquet, G.; Lecourtier, J.; Toulhoat, H. In *Physical Chemistry of Colloids and Interfaces in Oil Production*; Toulhoat, H., Lecourtier, J., Eds.; Editions Technip.: Paris, 1992; pp 275–278.
(25) Kirby, A. R.; Gunning, A. P.; Morris, V. J.; Ridout, M. J. *Biophys. J.* **1995**, *68*, 360–363.
(26) Kirby, A. R.; Gunning, A. P.; Morris, V. J. *Carbohydr. Res.* **1995**, *267*, 161–166.
(27) Yanaki, T.; Ito, W.; Tabata, K.; Kojima, T.; Norisuye, T.; Takano, N.; Fujita, H. *Biophys. Chem.* **1983**, *17*, 337–342.
(28) Misaki, A.; Kishida, E.; Kakuta, M.; Tabata, K. In *Carbohydrates and Carbohydrate Polymers: Analysis, Biotechnology, Modification, Antiviral, Biomedical and Other Applications*; Yalpani, M., Ed.; ATL Press, Inc.: Mount Prospect, 1993; Vol. 1; pp 116–129.
(29) Yanaki, T.; Norisuye, T. *Polym. J.* **1983**, *15*, 389–396.
(30) Norisuye, T. *Makromol. Chem., Suppl.* **1985**, *14*, 105–118.
(31) Stokke, B. T.; Brant, D. A. *Biopolymers* **1990**, *30*, 1161–1181.
(32) Stokke, B. T.; Elgsæter, A.; Hara, C.; Kitamura, S.; Takeo, S. *Biopolymers* **1993**, *33*, 561–573.
(33) Stokke, B. T.; Elgsæter, A. *Micron* **1994**, *25*, 469–491.
(34) Norisuye, T.; Yanaki, T.; Fujita, H. *J. Polym. Sci., Polym. Phys. Ed.* **1980**, *18*, 547–558.
(35) Sato, T.; Norisuye, T.; Fujita, H. *Carbohydr. Res.* **1981**, *95*, 195–204.
(36) Stokke, B. T.; Elgsæter, A.; Brant, D. A.; Kitamura, S. *Macromolecules* **1991**, *24*, 6349–6351.
(37) Stokke, B. T.; Elgsæter, A.; Brant, D. A.; Kitamura, S. In *Physical Chemistry of Colloids and Interfaces in Oil Production*; Toulhoat, H., Lecourtier, J., Eds.; Editions Technip.: Paris, 1992; pp 217–223.
(38) Stokke, B. T.; Elgsæter, A.; Brant, D. A.; Kuge, T.; Kitamura, S. *Biopolymers* **1993**, *33*, 193–198.
(39) Wang, J. C. In *Cyclic Polymers*; Semlyen, J. A., Ed.; Elsevier Applied Science: London, 1986; pp 225–260.
(40) Shore, D.; Baldwin, R. L. *J. Mol. Biol.* **1983**, *170*, 957–981.
(41) Kotera, A. In *Polymer Fractionation*; Cantow, M. J. R., Ed.; Academic Press: New York, 1967; pp 43–66.
(42) Kitamura, S.; Kuge, T. *Biopolymers* **1989**, *28*, 639–654.
(43) Tyler, J. M.; Branton, D. *J. Ultrastruct. Res.* **1980**, *71*, 95–102.
(44) Bluhm, T. L.; Deslandes, Y.; Marchessault, R. H.; Pérez, S.; Rinaudo, M. *Carbohydr. Res.* **1982**, *100*, 117–130.
(45) Parsegian, V. A. *Annu. Rev. Biophys. Bioeng.* **1973**, 2, 221–255.
(46) Murray, M. N.; Hansma, H. G.; Bezanilla, M.; Sano, T.; Ogletree, D. F.; Kolbe, W.; Smith, C. L.; Cantor, C. R.; Spengler, S.; Hansma, P. K.; Salmeron, M. *Proc. Natl. Acad. Sci. U.S.A.* **1993**, 90, 3811–3814.

MA950549W